

# Temperature-dependence of the static contact angle

A universal scaling law covering ideal cases,  
roughness effects and the transition to total wetting



Normandie Université

**Benoît Duchemin, Guillaume Cazaux,  
Moussa Gomina, Joël Bréard**

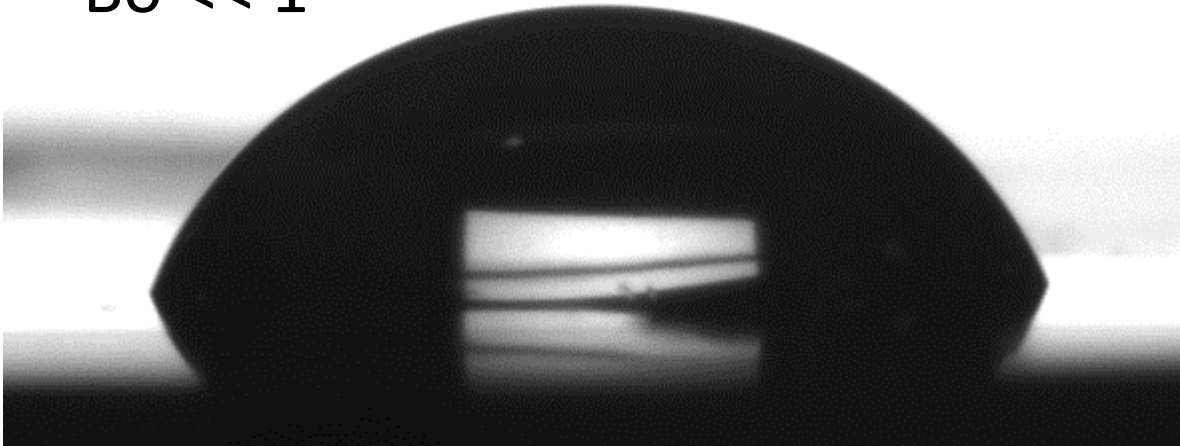
**Laboratoire Ondes et Milieux Complexes  
Normandie Université, CNRS**

**LE HAVRE, FRANCE**

***ACS spring 2021 national meeting***

# Static contact angles are ubiquitous

- A liquid standing on a solid surface
- Importance in many technological fields: coatings, composites, kitchenware, automotive industry, etc.
- $Bo \ll 1$

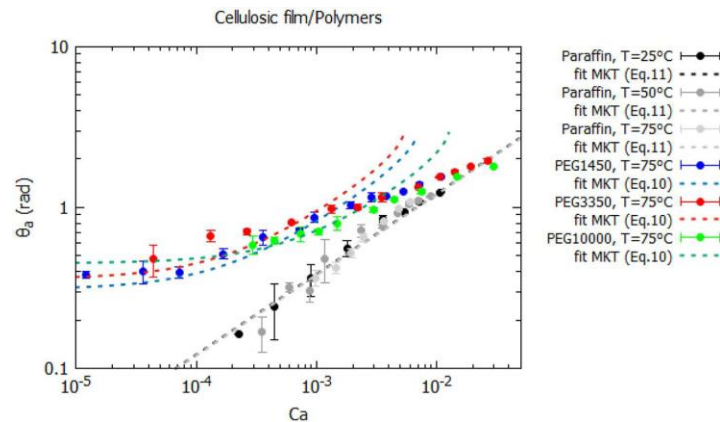


# Effect of temperature on contact angles

The case of dynamic contact angles is « covered » by two main theories

The molecular kinetic theory (Blake and Haynes, 1969)

$$v = 2K_0\lambda \sinh\left[\frac{\gamma\lambda^2(\cos\theta_e - \cos\theta_d)}{2k_B T}\right]$$



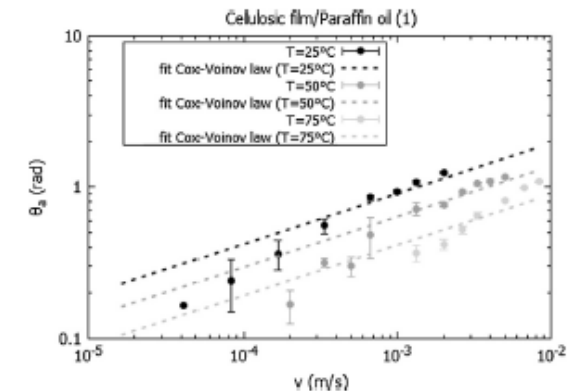
The hydrodynamic approaches

Tanner (1979)-De Gennes (1986)

$$\theta_d(\theta_d^2 - \theta_e^2) = 6\Gamma Ca$$

Cox (1962)-Voinov (1976)

$$\theta_d^3 - \theta_e^3 = 9\Gamma Ca$$



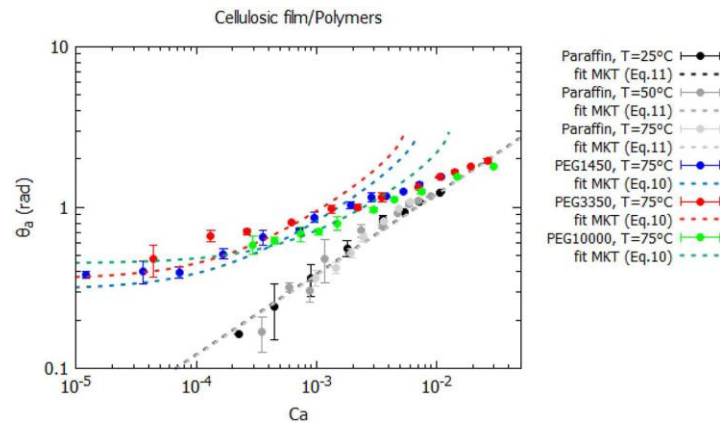
Pucci, M.F., Duchemin, B., Gomina, M., Bréard, J., 2020. Dynamic Wetting of Molten Polymers on Cellulosic Substrates: Model Prediction for Total and Partial Wetting. *Front. Mater.* 7, 143.  
 Pucci, M.F., Duchemin, B., Gomina, M., Bréard, J., 2018. Temperature effect on dynamic wetting of cellulosic substrates by molten polymers for composite processing. *Composites Part A: Applied Science and Manufacturing* 114, 307–315.

# Effect of temperature on contact angles

The case of dynamic contact angles is « covered » by two main theories

The molecular kinetic theory (Blake and Haynes, 1969)

$$v = 2K_0 \lambda \sinh \left[ \frac{\gamma \ell^2 (\cos \theta_e - \cos \theta_d)}{2k_B T} \right]$$



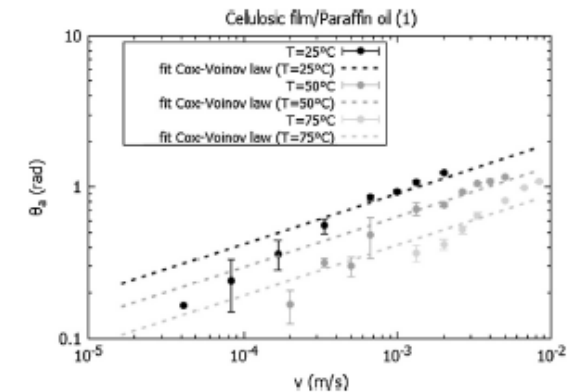
The hydrodynamic approaches

Tanner (1979)-De Gennes (1986)

$$\theta_d (\theta_d^2 - \theta_e^2) = 6\Gamma Ca$$

Cox (1962)-Voinov (1976)

$$\theta_d^3 - \theta_e^3 = 9\Gamma Ca$$



- Pucci, M.F., Duchemin, B., Gomina, M., Bréard, J., 2020. Dynamic Wetting of Molten Polymers on Cellulosic Substrates: Model Prediction for Total and Partial Wetting. *Front. Mater.* 7, 143.
- Pucci, M.F., Duchemin, B., Gomina, M., Bréard, J., 2018. Temperature effect on dynamic wetting of cellulosic substrates by molten polymers for composite processing. *Composites Part A: Applied Science and Manufacturing* 114, 307–315.

# Effect of temperature on static contact angles

The case of *static* contact angles is less clear :

- $\Theta = a.T + b$  (De Ruijter, 1988; Petke, 1969)
- $\cos(\Theta) = a.T + b$  (Gribanova, 1992; Zisman, 1964)
- $\cos(\Theta) = a.T^x + b$  (Bernardin, 1997; Adamson, 1973)
- One case of  $\nearrow \theta$  with  $\nearrow T$  (Berim, 2009)

The question of a universal and predictive model remains...

spreads on a surface as a function of temperature ( $\rightarrow \theta(T)$ ).

**Hypothesis 1:** Break down the surface energy into a dispersive and a polar component and use it as a prediction tool

Van Oss, Good and Chaudury (1986, 1988):

$$\gamma = \gamma^{LW} + \gamma^{AB}$$

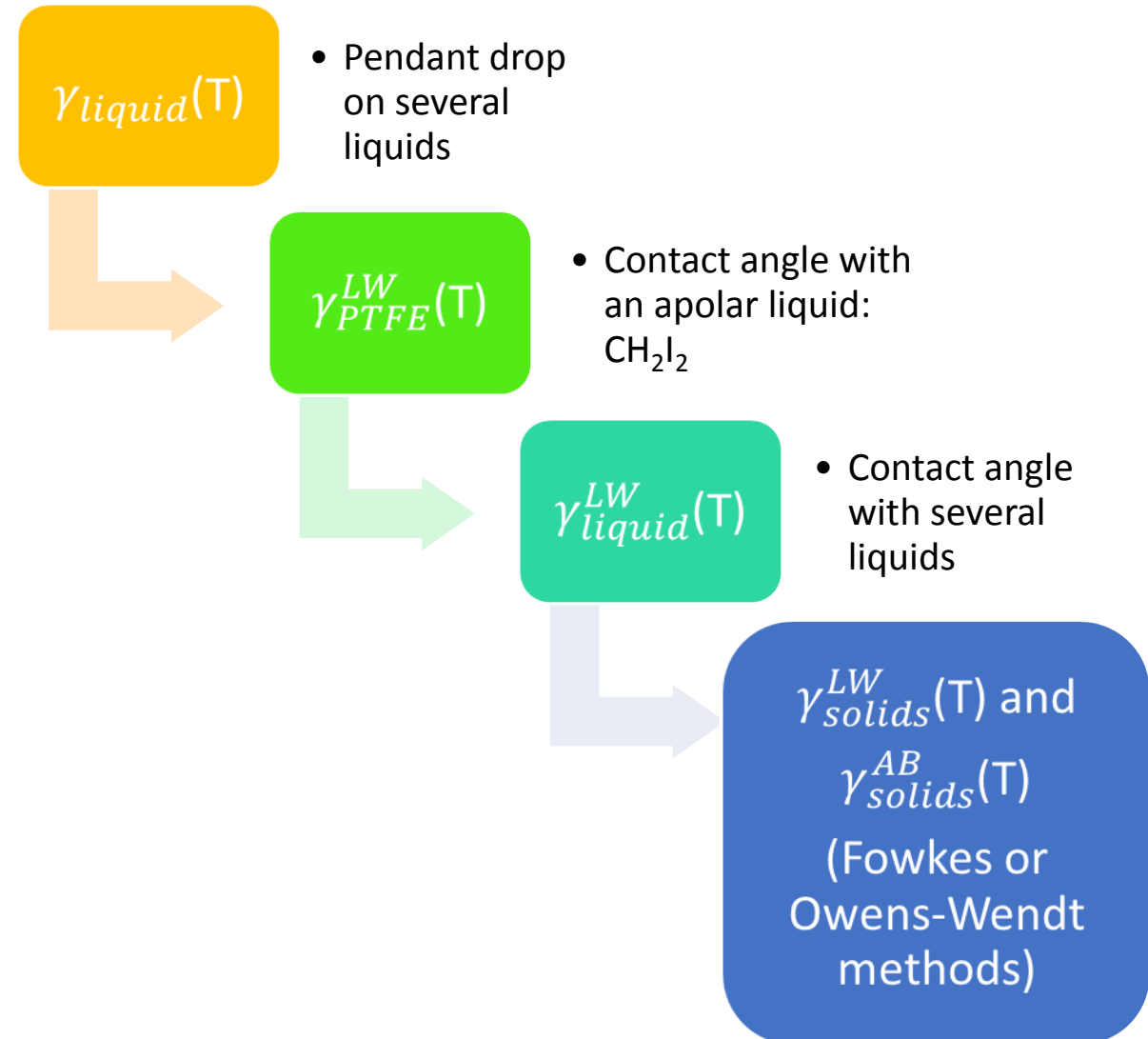
The Berthelot hypothesis when at least one component is apolar:

$$\gamma_{solid-liquid} = \gamma_{solid} + \gamma_{liquid} - 2 \cdot (\gamma_{solid}^{LW} \cdot \gamma_{liquid}^{LW})^{1/2}$$

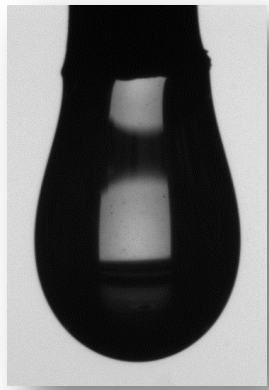
Which mixed with Young's equation and neglecting the spreading pressure gives:

$$\gamma_{liquid} \cdot (1 + \cos \theta_s) = 2 \cdot (\gamma_{solid}^{LW} \cdot \gamma_{liquid}^{LW})^{1/2}$$

## Method:



Eötvös (1886):  
 $\gamma_l \cdot V_m^{2/3} = \kappa \cdot (T_0 - T)$



**Method:**

$\gamma_{liquid}(T)$

- Pendant drop on several liquids

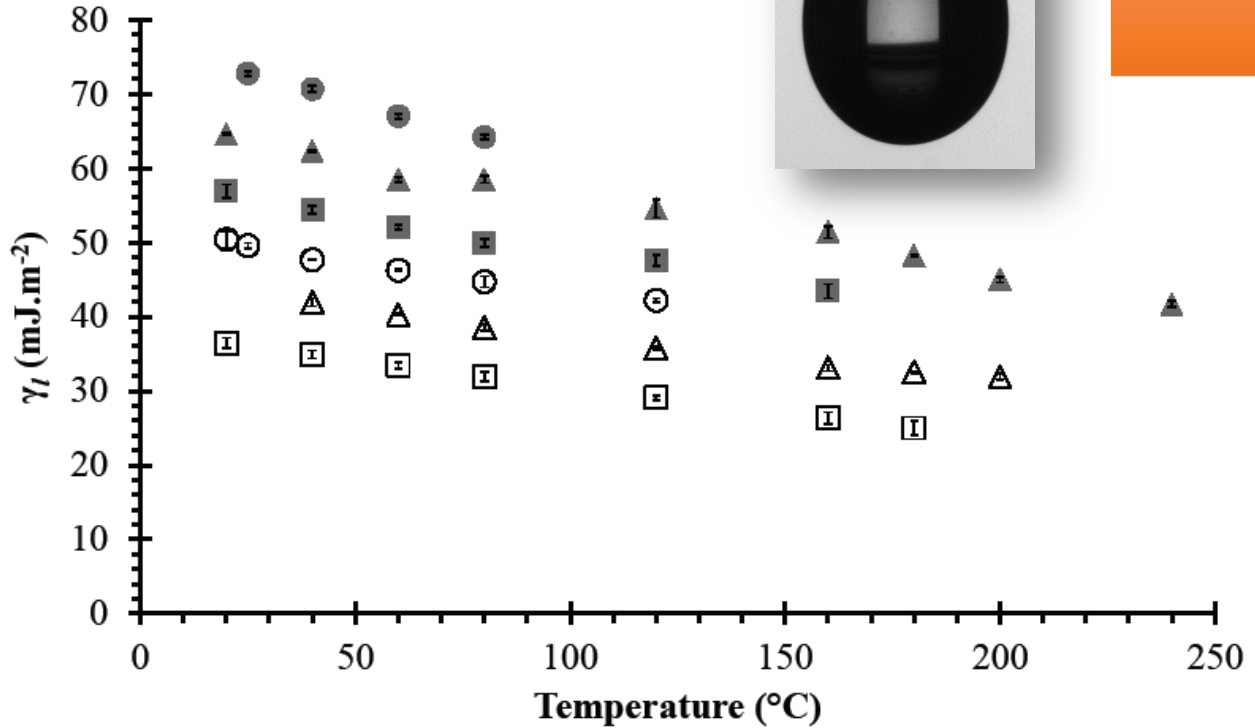
$\gamma_{PTFE}^{LW}(T)$

- Contact angle with an apolar liquid:  $CH_2I_2$

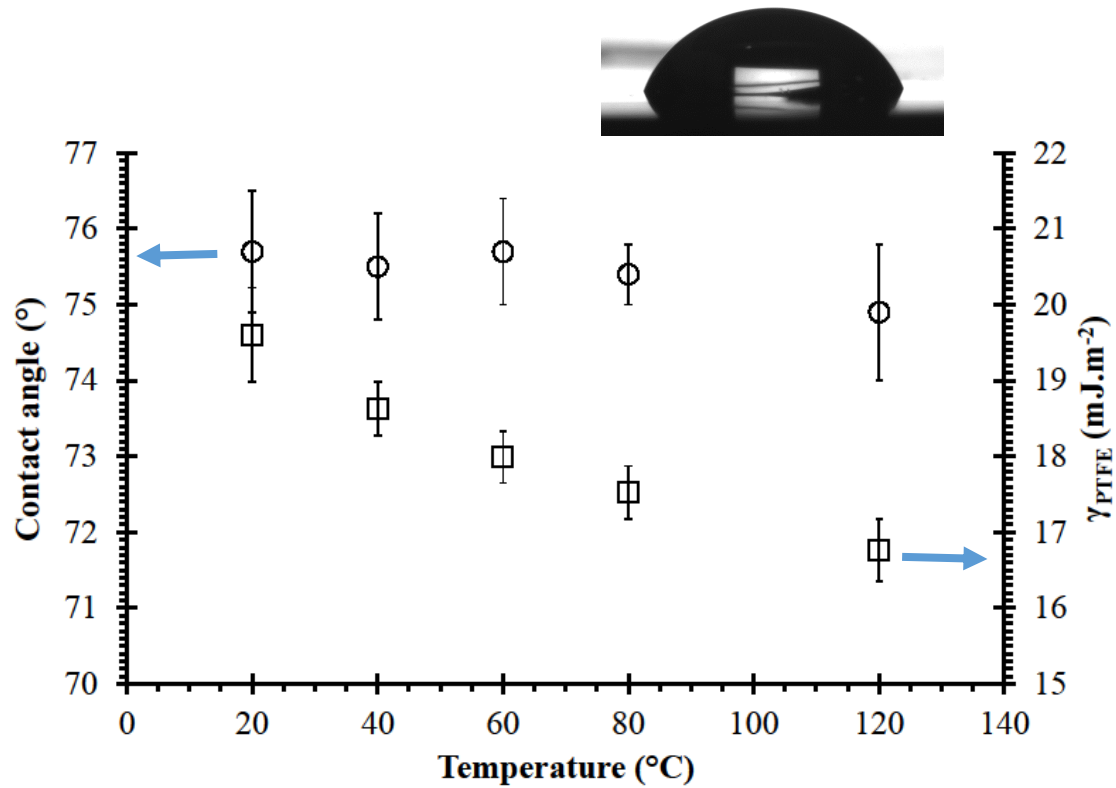
$\gamma_{liquid}^{LW}(T)$

- Contact angle with several liquids

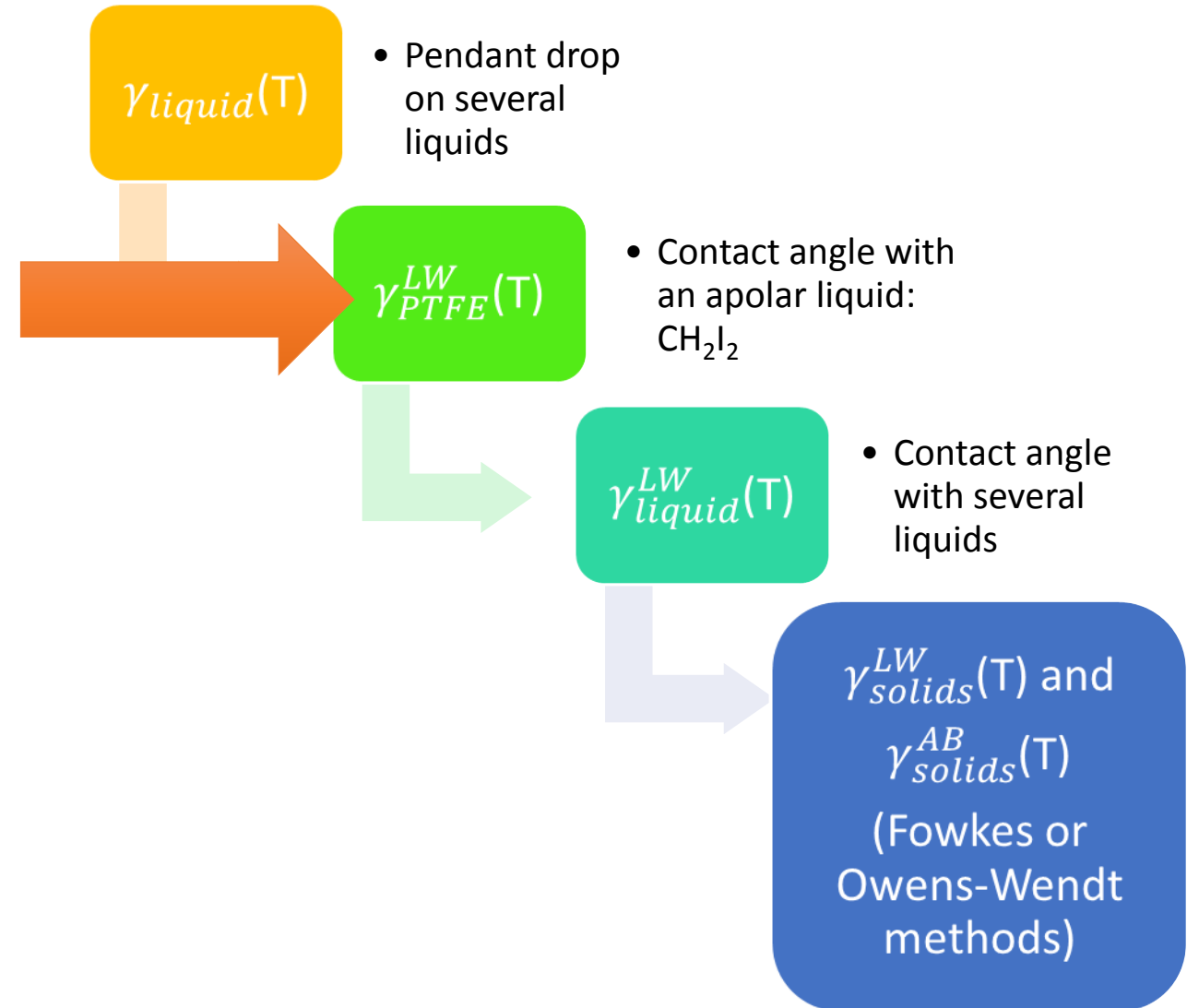
$\gamma_{solids}^{LW}(T)$  and  $\gamma_{solids}^{AB}(T)$   
 (Fowkes or Owens-Wendt methods)



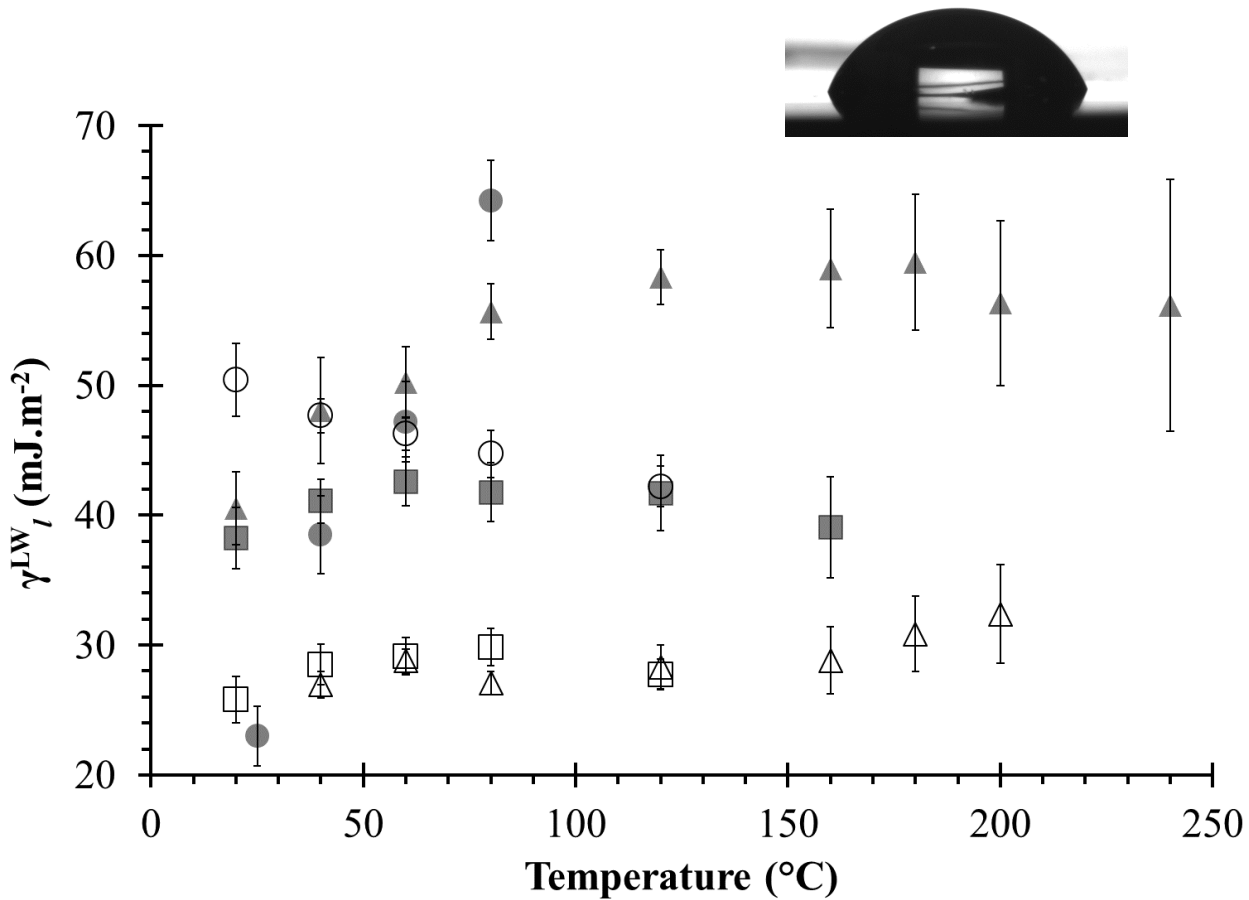
Surface tensions of water (●), glycerol (▲),  
 formamide (■), methylene iodide (○), ethylene  
 carbonate (△) and methyl benzoate (□) at various  
 temperatures.



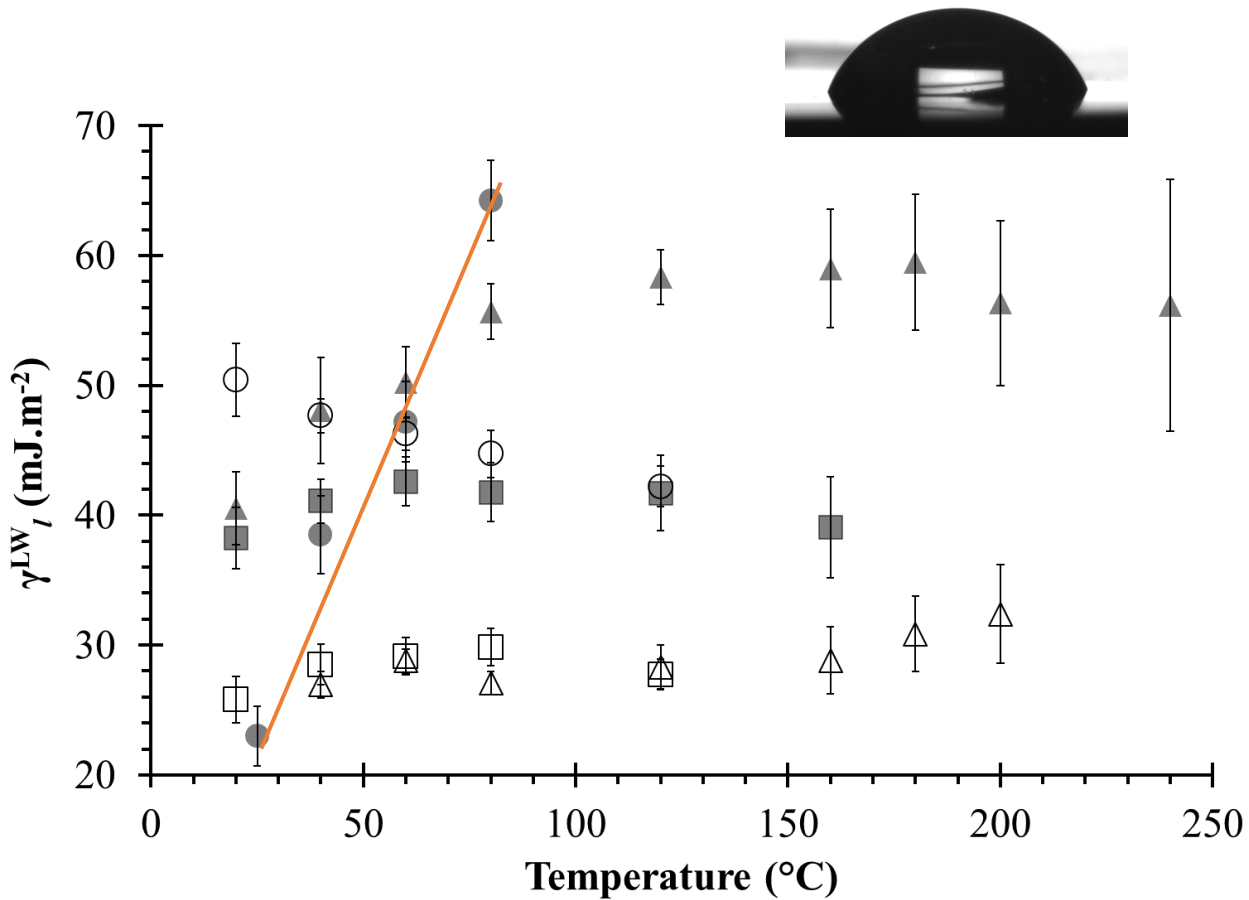
## Method:





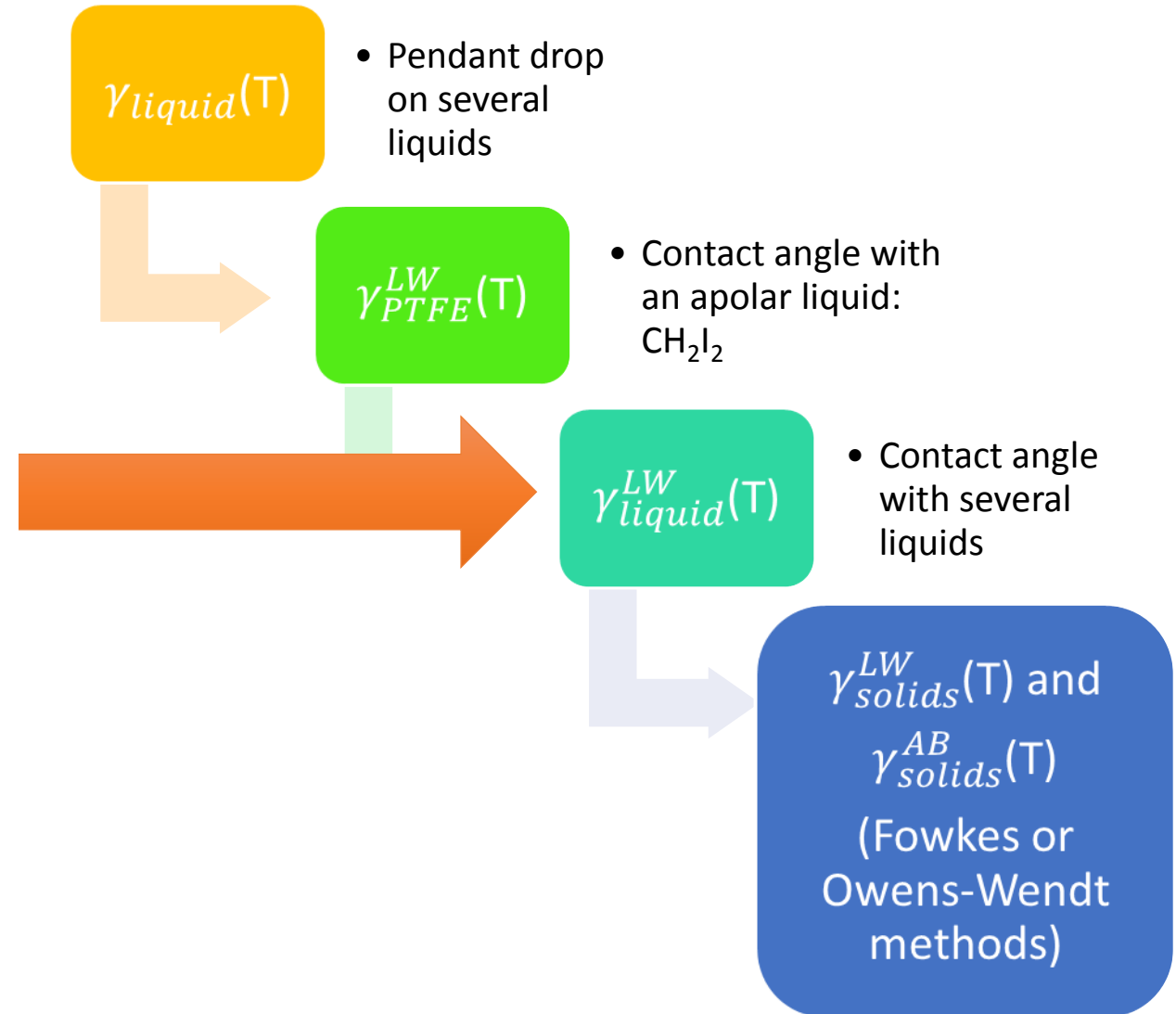


Calculated dispersive components of the surface tensions of water (●), glycerol (▲), formamide (■), methylene iodide (○), ethylene carbonate (△) and methyl benzoate (□) at various temperatures. All error bars were calculated by propagation of uncertainty.



Calculated dispersive components of the surface tensions of water (●), glycerol (▲), formamide (■), methylene iodide (○), ethylene carbonate (△) and methyl benzoate (□) at various temperatures. All error bars were calculated by propagation of uncertainty.

## Method:



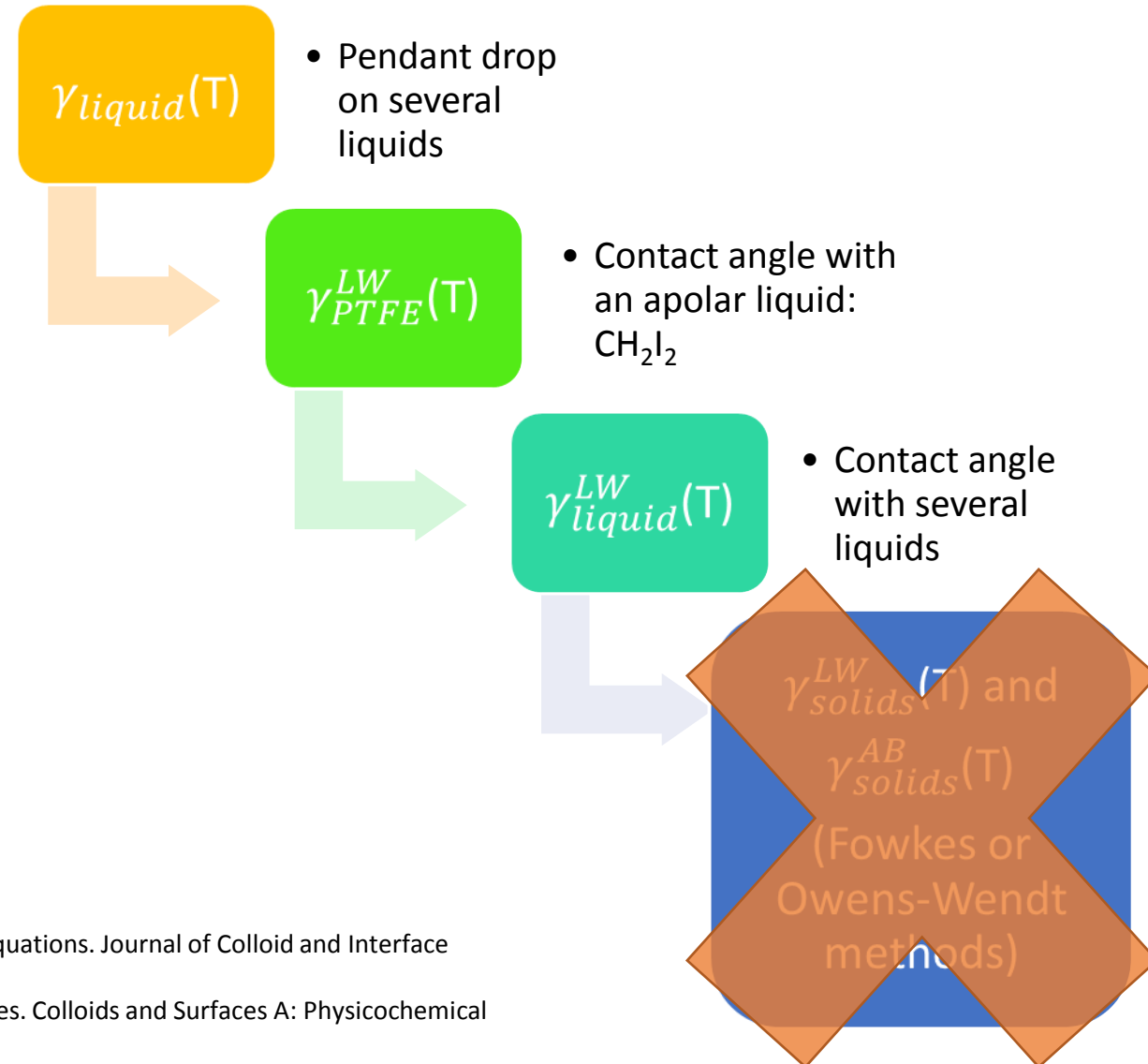
## Conclusion:

The matter comes from  $\gamma$  and Berthelot's hypothesis:  $\gamma$  is a thermodynamic quantity (Helmholtz energy) but the interaction term  $(\gamma_{solid}^{LW} \cdot \gamma_{liquid}^{LW})^{1/2}$  is formulated as if it were temperature independent (because  $\gamma^{LW}$  is athermal).

In other words, the entropic part of the interaction has been neglected.

This problem has been mentioned several times and probably overlooked due to the use of this formula at constant temperature (RT), inducing self-consistency.

## Method:



**Douillard, J.M., 1997.** Concerning the Thermodynamic Consistency of the "Surface Tension Components" Equations. *Journal of Colloid and Interface Science* 188, 511–515.

**Lyklema, J., 1999.** The surface tension of pure liquids: Thermodynamic components and corresponding states. *Colloids and Surfaces A: Physicochemical and Engineering Aspects* 156, 413–421.

**Weber, C., Stanjek, H., 2014.** Energetic and entropic contributions to the work of adhesion in two-component, three-phase solid–liquid–vapour systems. *Colloids and Surfaces A: Physicochemical and Engineering Aspects* 441, 331–339.

# A physical description based on the thermocapillary amplitude

Following the demonstration by Blake and Haynes:  
The rate constant of a liquid molecule jumping forward and that of a molecule jumping backward around the triple line are equal:

$$k_{des} = k_{ads}$$

Therefore:

$$\frac{F_{ads}^\ddagger}{F_{des}^\ddagger} = e^{\frac{-(E_{ads} - E_{des})}{k_B T}}$$

Activation free energy

Partition function ratio (similar to Crooks definition of entropy: the probability of undergoing a process divided by the probability of undergoing the reverse process)

# A physical description based on the thermocapillary amplitude

Following the demonstration by Blake and Haynes:  
The rate constant of a liquid molecule jumping forward and that of a molecule jumping backward around the triple line are equal:

$$k_{des} = k_{ads}$$

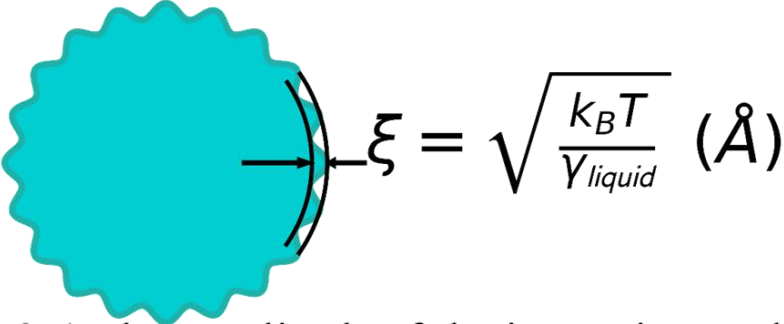
Therefore:

$$\frac{F_{ads}^\ddagger}{F_{des}^\ddagger} = e^{-\frac{(E_{ads} - E_{des})}{k_B T}}$$

Activation free energy

Partition function ratio (similar to Crooks definition of entropy: the probability of undergoing a process divided by the probability of undergoing the reverse process)

The surface of liquids bears a certain roughness due to the existence of thermally excited capillary waves. The scale of the problem is the thermal length  $\xi$ :



$$\xi = \sqrt{\frac{k_B T}{\gamma_{liquid}}} \text{ (\AA)}$$

**Hypothesis 2-1:** the amplitude of the jumps is equal to  $\xi$ :

$$E_{ads} - E_{des} = -S \cdot \xi^2$$

Where  $S$  is the spreading parameter:

$$S = \gamma_{sv} - (\gamma_{sl} + \gamma_l)$$

$$S = \gamma_l (\cos \theta_Y - 1)$$

# A physical description based on the thermocapillary amplitude

Following the demonstration by Blake and Haynes:  
The rate constant of a liquid molecule jumping forward and that of a molecule jumping backward around the triple line are equal:

Therefore:

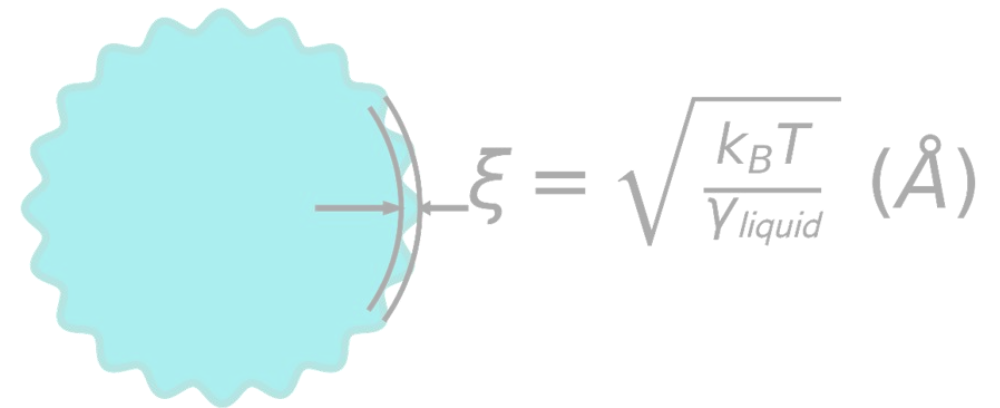
$$\frac{F_{ads}^\ddagger}{F_{des}^\ddagger} = e^{\frac{\gamma_l(\cos\theta - 1)\xi^2}{k_B T}} = e^{\cos\theta - 1}$$

$k_{des} = k_{ads}$

Activation free energy

Partition function ratio (similar to Crooks definition of entropy: the probability of undergoing a process divided by the probability of undergoing the reverse process)

Thermal length  $\xi$ :



$$E_{ads} - E_{des} = -\gamma_l(\cos\theta_Y - 1) \cdot \xi^2$$

# A physical description based on the thermocapillary amplitude

Following the demonstration by Blake and Haynes:  
The rate constant of a liquid molecule jumping forward and that of a molecule jumping backward around the triple line are equal:

Therefore:

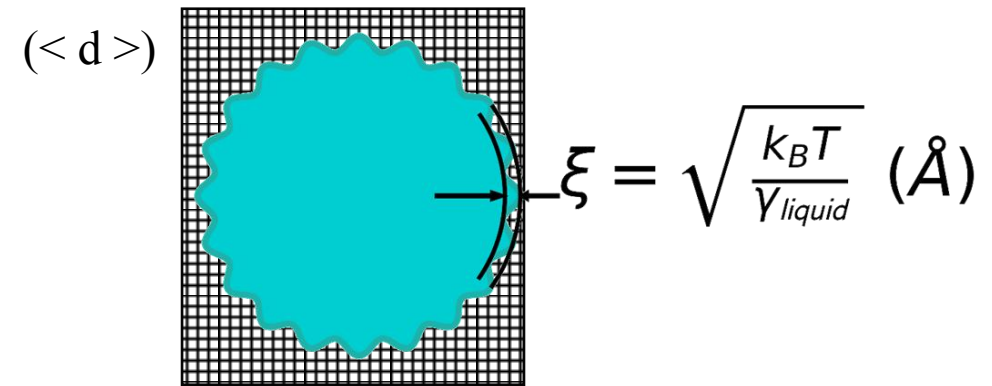
$$\frac{F_{ads}^\ddagger}{F_{des}^\ddagger} = e^{-\frac{\gamma_l(\cos\theta-1)\xi^2}{k_B T}} = e^{\cos\theta-1}$$

$k_{des} = k_{ads}$

Activation free energy

Partition function ratio (similar to Crooks definition of entropy: the probability of undergoing a process divided by the probability of undergoing the reverse process)

A characteristic distance ( $\langle d \rangle$ ) understood as the lateral correlation length between adsorption sites (or finite potential wells) describes the pseudo-periodicity of the surface:



Hypothesis 2-2: The partition function ratio is assumed to be equal to the ratio of capillary wave amplitude divided by this cutoff length, with a fractal dimension:

$$\frac{F_{ads}^\ddagger}{F_{des}^\ddagger} = \left(\frac{\xi}{\langle d \rangle}\right)^f$$

# A physical description based on the thermocapillary amplitude

Following the demonstration by Blake and Haynes:  
The rate constant of a liquid molecule jumping forward and that of a molecule jumping backward around the triple line are equal:

$$k_{des} = k_{ads}$$

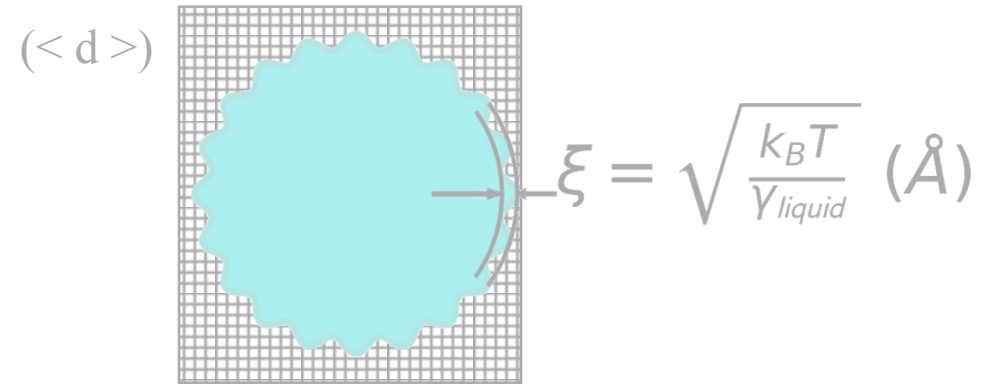
Therefore:

$$\left( \frac{\xi}{\langle d \rangle} \right)^f = e^{\cos \theta - 1}$$

When  $T \nearrow$ ,  $\xi \nearrow$ .

When  $\xi = \langle d \rangle$ , a thermal transition to total wetting is induced.

A characteristic distance ( $\langle d \rangle$ ) understood as the lateral correlation length between adsorption sites (or finite potential wells) describes the pseudo-periodicity of the surface:



Hypothesis 2-2: The partition function ratio is assumed to be equal to the ratio of capillary wave amplitude divided by this cutoff length, with a fractal dimension:

$$\frac{F_{ads}^\ddagger}{F_{des}^\ddagger} = \left( \frac{\xi}{\langle d \rangle} \right)^f$$



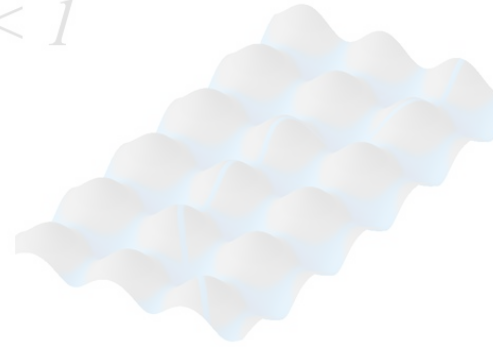
# A physical description based on the thermocapillary amplitude

$$\left(\frac{\xi}{\langle d \rangle}\right)^f = e^{\cos \theta - 1}$$

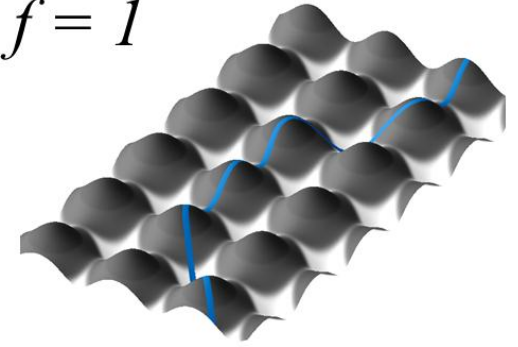
Where  $f$  is the fractal dimension of the problem:

- $f = 1$  for a triple line jumping straight from well to well

$f < 1$



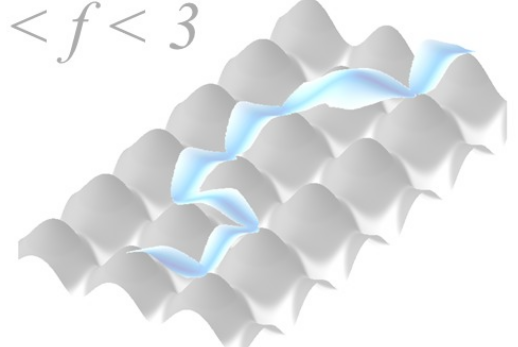
$f = 1$



$1 < f < 2$



$2 < f < 3$



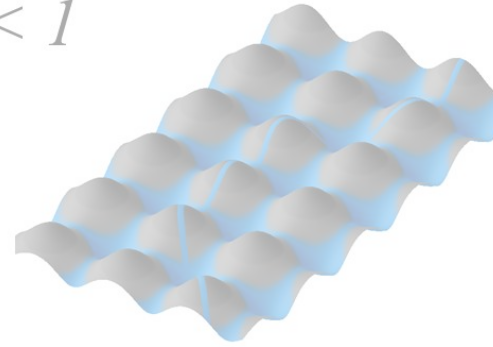
# A physical description based on the thermocapillary amplitude

$$\left(\frac{\xi}{\langle d \rangle}\right)^f = e^{\cos \theta - 1}$$

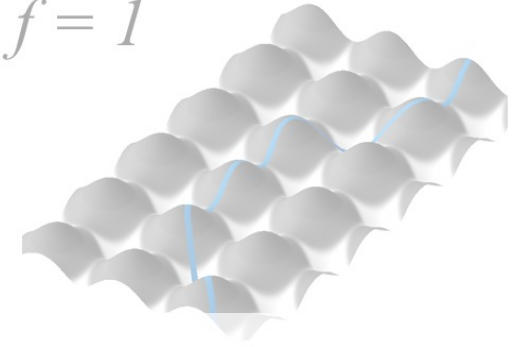
Where  $f$  is the fractal dimension of the problem:

- $f = 1$  for a triple line jumping straight from well to well,
- $1 \leq f < 2$  for a “normal” triple line thermally fluctuating

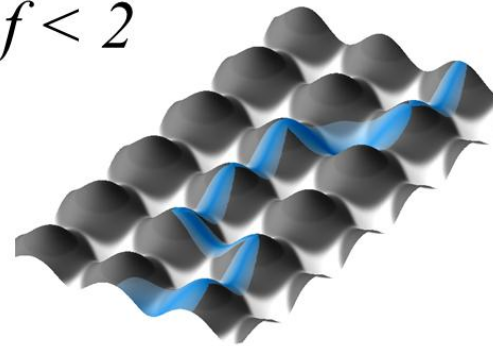
$f < 1$



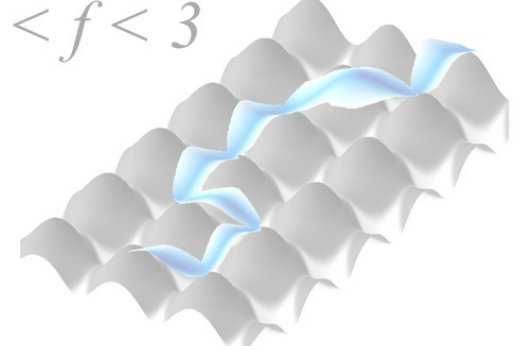
$f = 1$



$1 < f < 2$



$2 < f < 3$



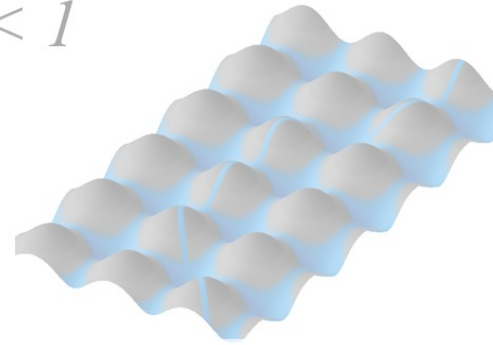
# A physical description based on the thermocapillary amplitude

$$\left(\frac{\xi}{\langle d \rangle}\right)^f = e^{\cos \theta - 1}$$

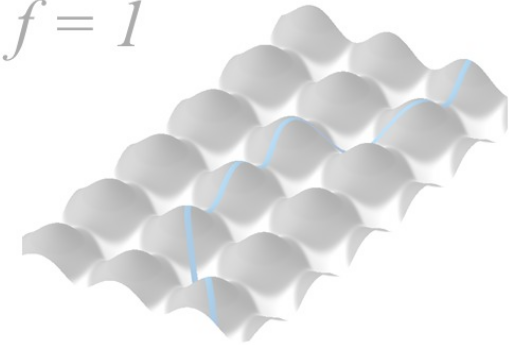
Where  $f$  is the fractal dimension of the problem:

- $f = 1$  for a triple line jumping straight from well to well,
- $1 \leq f < 2$  for a “normal” triple line thermally fluctuating
- $2 \leq f < 3$  for a planar triple line, i.e. a Cassie-Baxter state with entrapped gas between the solid surface and the liquid

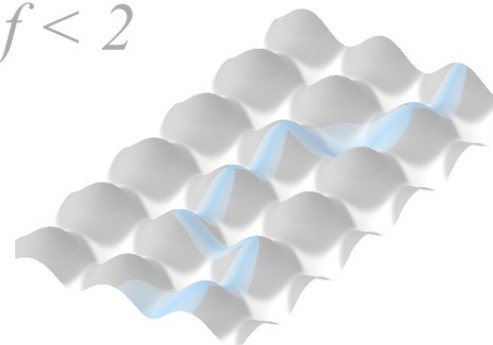
$f < 1$



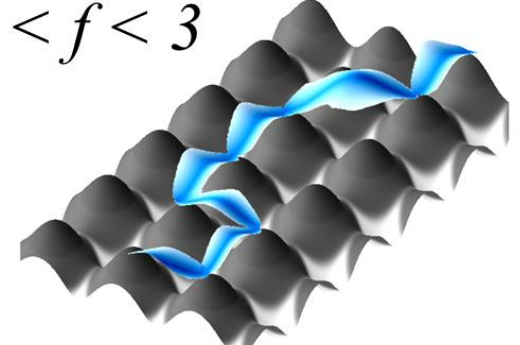
$f = 1$



$1 < f < 2$



$2 < f < 3$



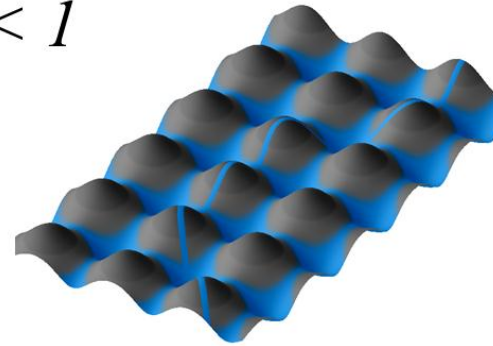
# A physical description based on the thermocapillary amplitude

$$\left(\frac{\xi}{\langle d \rangle}\right)^f = e^{\cos \theta - 1}$$

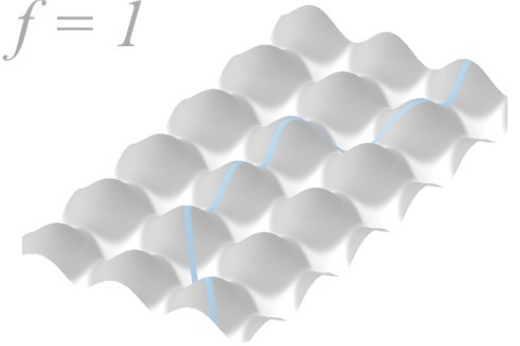
Where  $f$  is the fractal dimension of the problem:

- $f = 1$  for a triple line jumping straight from well to well,
- $1 \leq f < 2$  for a “normal” triple line thermally fluctuating
- $2 \leq f < 3$  for a planar triple line, i.e. a Cassie-Baxter state with entrapped gas between the solid surface and the liquid
- $f < 1$  if “hemiwicking” takes place (Wenzel state), thereby decreasing the fraction of triple line in contact with the solid.

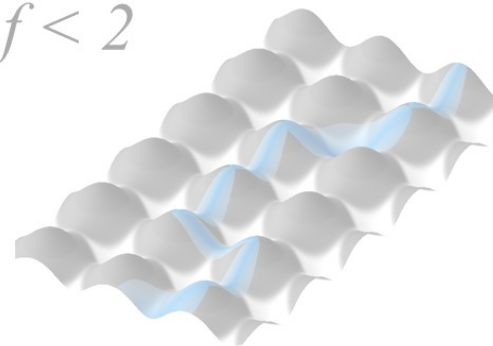
$f < 1$



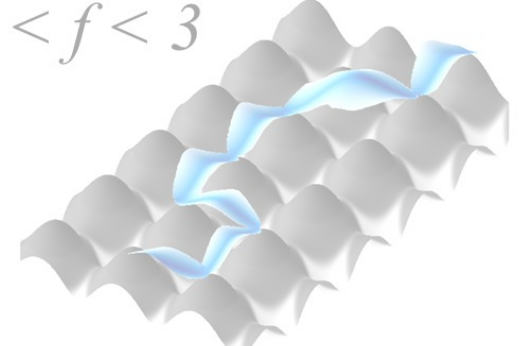
$f = 1$



$1 < f < 2$



$2 < f < 3$

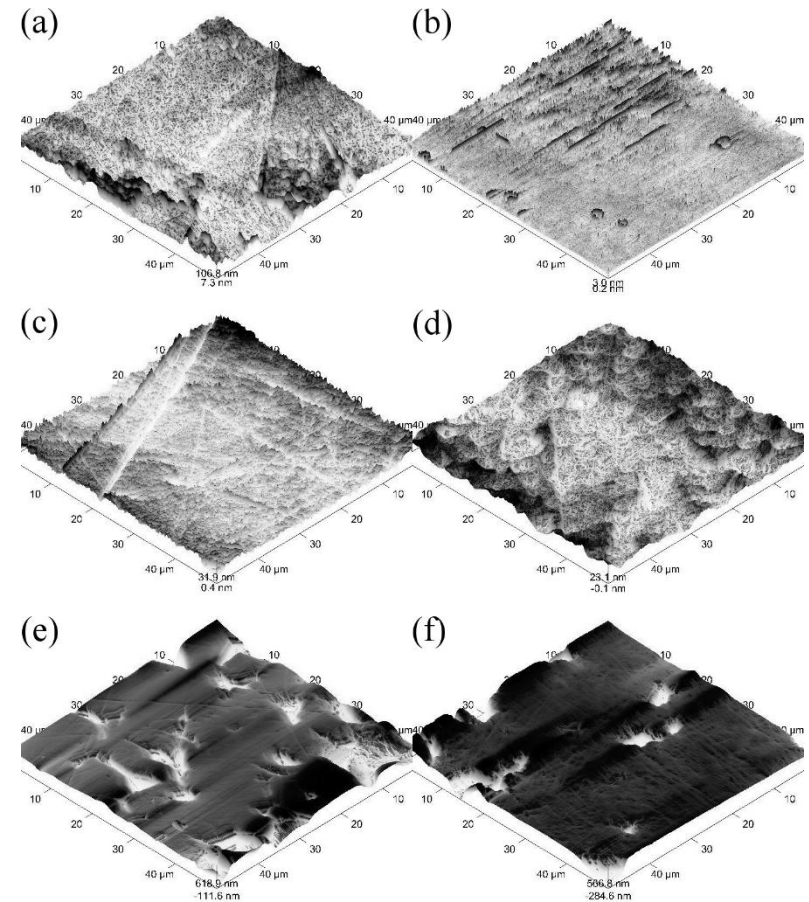


# Experimental validation

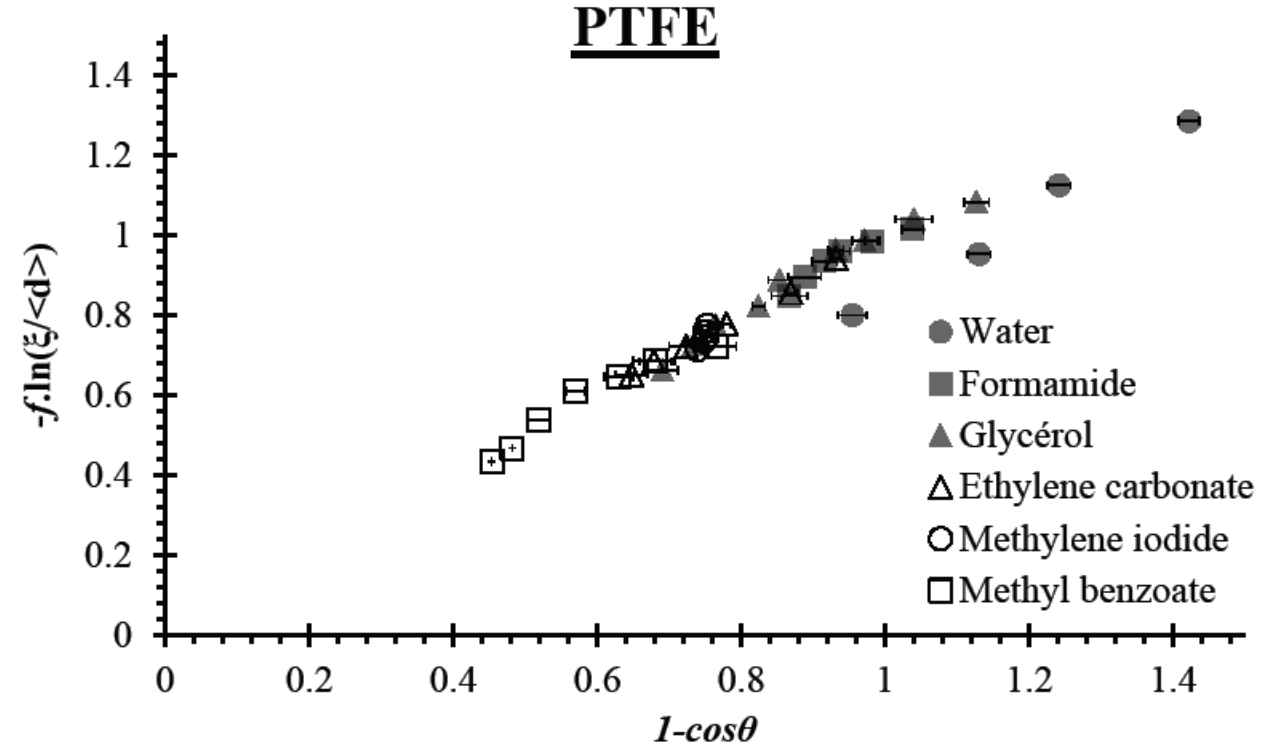
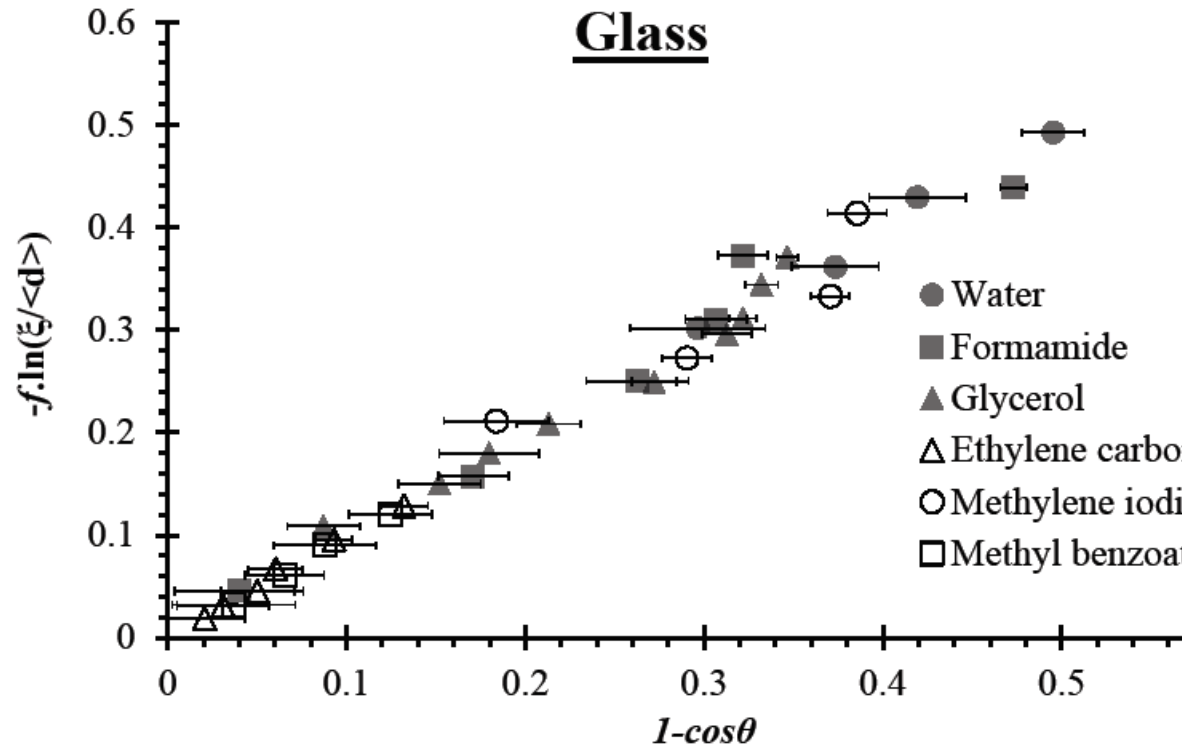
**Six liquids:** water, glycerol, methylene iodide, formamide, ethylene carbonate and methyl benzoate.

**Six solids:** (a) PTFE, (b) glass, (c) brass, (d) stainless steel, (e) alumina and (f) yttria-stabilized zirconia.

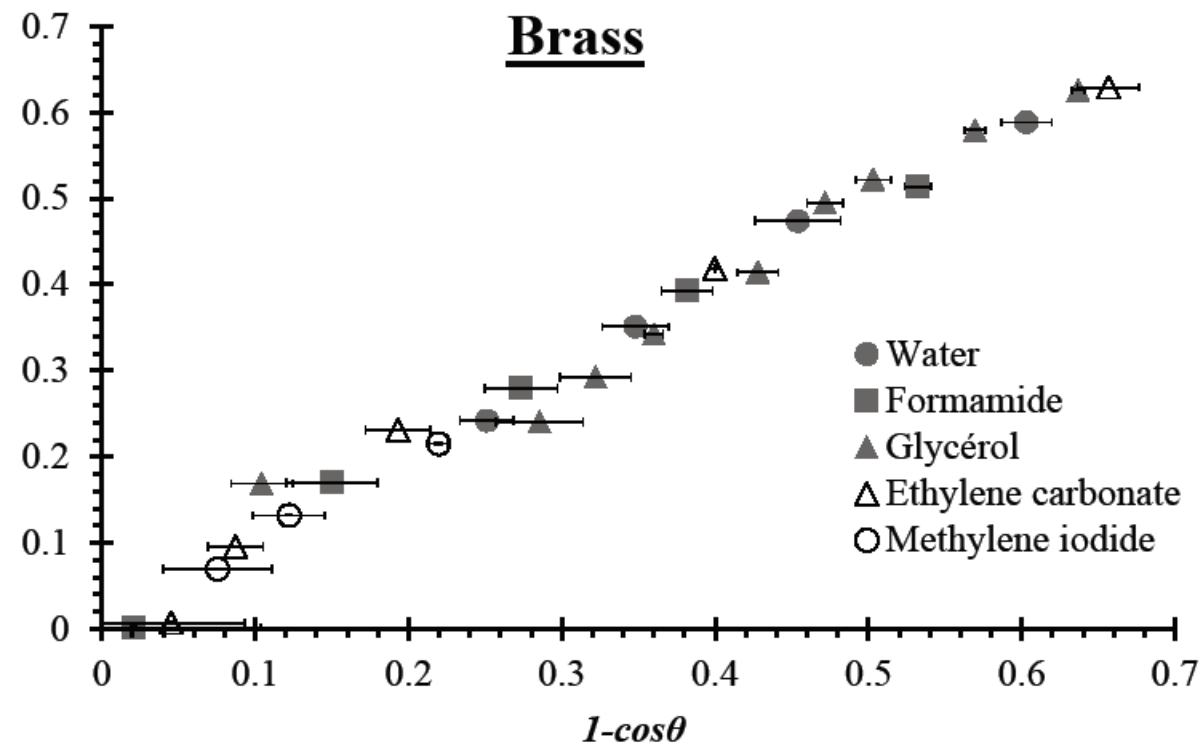
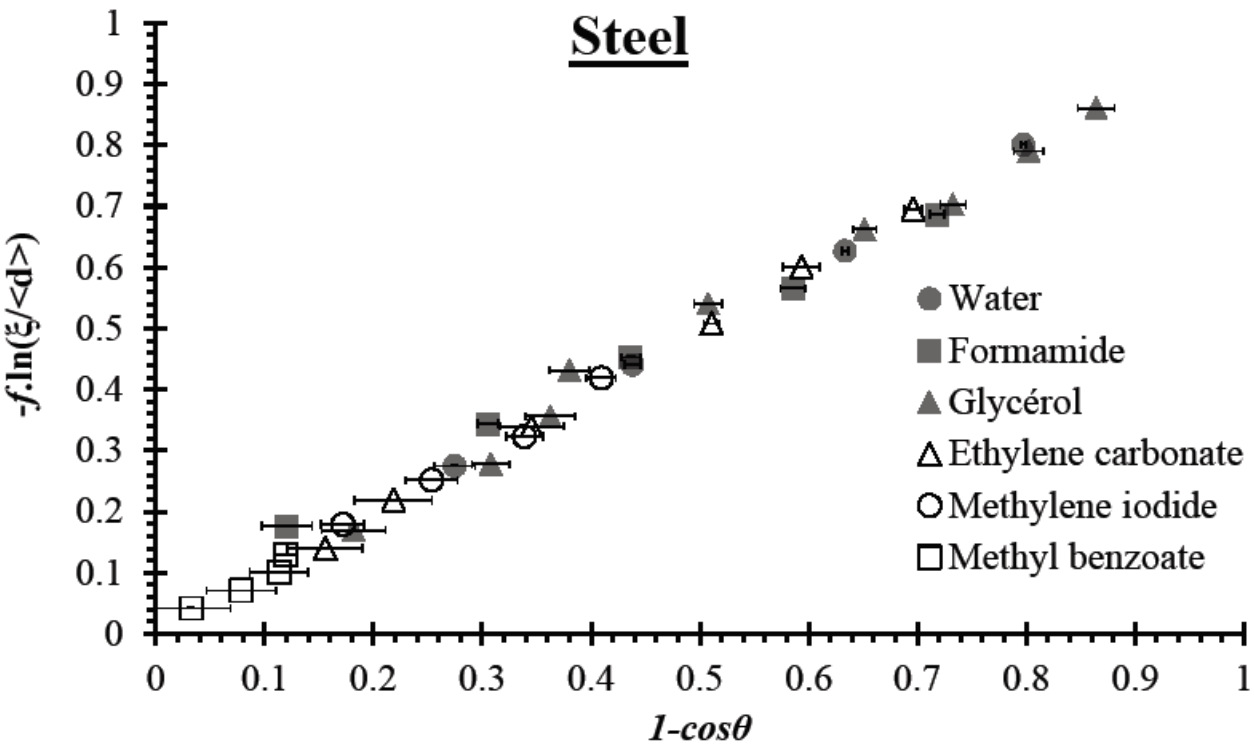
**Temperature range:** between 20 and 240°C.



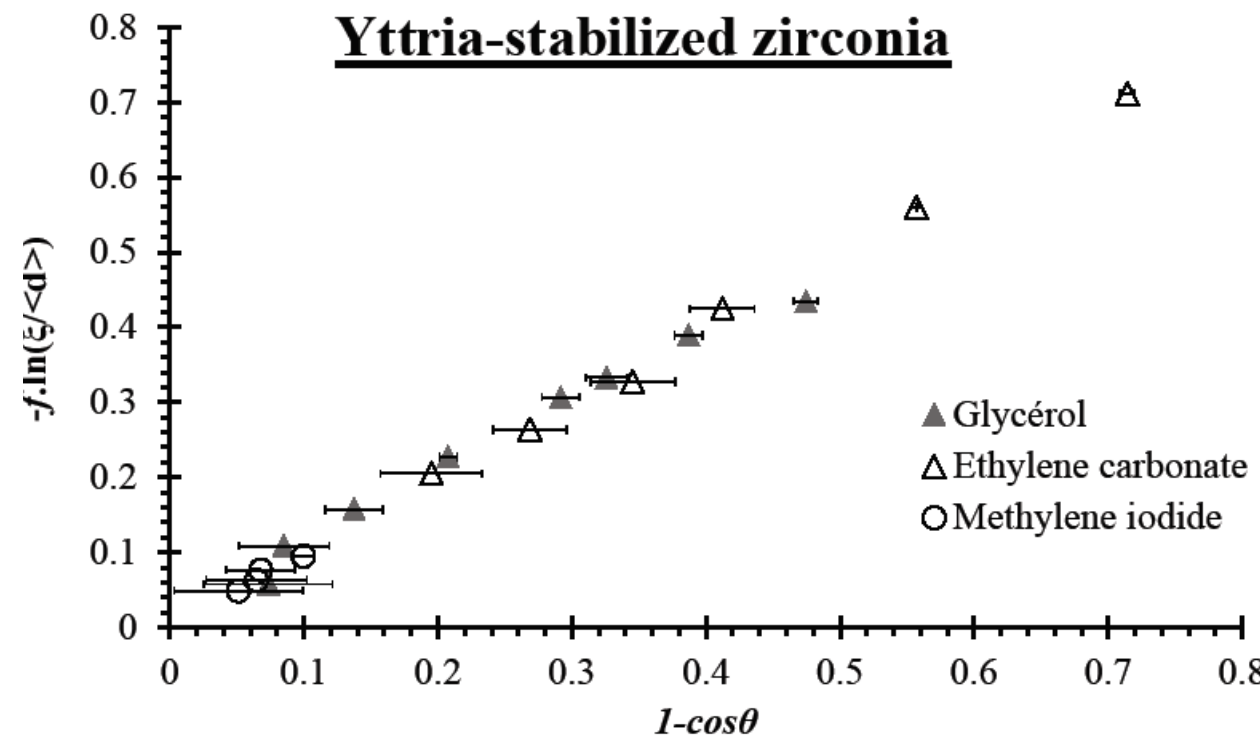
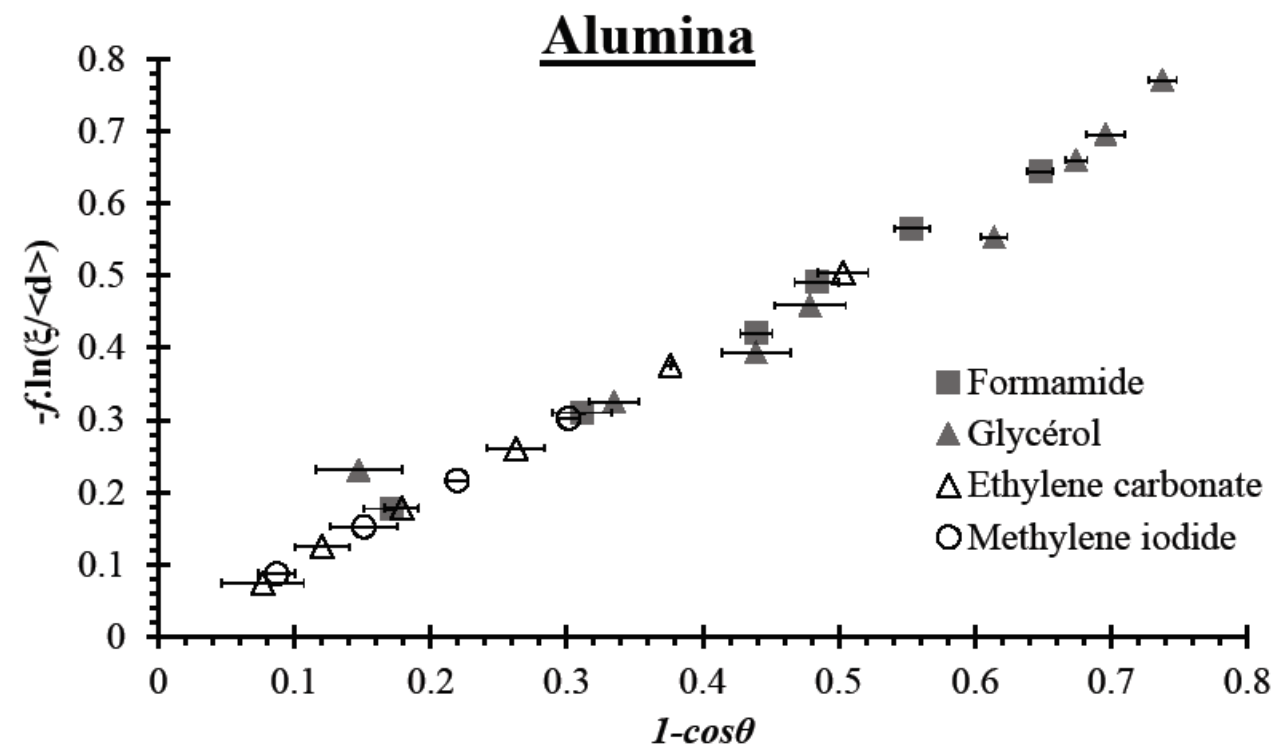
# Validation (1/3)



# Validation (2/3)



# Validation (3/3)





# Discussion

Substrate	Parameters	Water	Formamide	Glycerol	Ethylene carbonate	Methylene iodide	Methyl benzoate
Glass	$f$	1.18	1.19	0.53	0.32	1.32	0.56
	$\langle d \rangle (\text{\AA})$	3.56	3.86	5.07	4.80	3.87	4.14
	$R^2$	0.9870	0.9619	0.9683	0.9902	0.8724	0.9863
PTFE	$f$	3.00	0.50	0.84	0.85	0.26	0.71
	$\langle d \rangle (\text{\AA})$	3.60	20.09	9.06	9.73	56.03	9.19
	$R^2$	0.9886	0.9069	0.9695	0.9941	0.7488	0.9375
Stainless steel	$f$	3.25	2.16	1.38	1.83	1.57	0.56
	$\langle d \rangle (\text{\AA})$	3.00	3.67	4.66	4.69	3.70	4.21
	$R^2$	0.9996	0.9716	0.9871	0.9983	0.9880	0.9076
Brass	$f$	2.14	2.16	0.92	2.05	1.36	0.19
	$\langle d \rangle (\text{\AA})$	3.09	3.38	4.96	4.36	3.32	4.33
	$R^2$	0.9898	0.9920	0.9584	0.9841	0.9862	1 (*)
Alumina	$f$	n.a.	1.41	1.20	1.25	1.41	0.09
	$\langle d \rangle (\text{\AA})$	n.a.	4.21	4.99	4.80	3.51	4.96
	$R^2$	n.a.	0.9957	0.9561	0.9998	0.9995	1(*)
Zirconia	$f$	n.a.	n.a.	0.90	1.48	0.30	n.a.
	$\langle d \rangle (\text{\AA})$	n.a.	n.a.	4.06	5.20	3.88	n.a.
	$R^2$	n.a.	n.a.	0.9774	0.9967	0.9139	n.a.

# Discussion

Substrate	Parameters	Water	Formamide	Glycerol	Ethylene carbonate	Methylene iodide	Methyl benzoate
Glass	$f$	1.18	1.19	0.53	0.32	1.32	0.56
	$\langle d \rangle (\text{\AA})$	3.56	3.86	5.07	4.80	3.87	4.14
	$R^2$	0.9870	0.9619	0.9683	0.9902	0.8724	0.9863
PTFE	$f$	3.00	0.50	0.84	0.85	0.26	0.71
	$\langle d \rangle (\text{\AA})$	3.60	20.09	9.06	9.73	56.03	9.19
	$R^2$	0.9886	0.9069	0.9695	0.9941	0.7488	0.9375
Stainless steel	$f$	3.25	2.16	1.38	1.83	1.57	0.56
	$\langle d \rangle (\text{\AA})$	3.00	3.67	4.66	4.69	3.70	4.21
	$R^2$	0.9996	0.9716	0.9871	0.9983	0.9880	0.9076
Brass	$f$	2.14	2.16	0.92	2.05	1.36	0.19
	$\langle d \rangle (\text{\AA})$	3.09	3.38	4.96	4.36	3.32	4.33
	$R^2$	0.9898	0.9920	0.9584	0.9841	0.9862	1 (*)
Alumina	$f$	n.a.	1.41	1.20	1.25	1.41	0.09
	$\langle d \rangle (\text{\AA})$	n.a.	4.21	4.99	4.80	3.51	4.96
	$R^2$	n.a.	0.9957	0.9561	0.9998	0.9995	1(*)
Zirconia	$f$	n.a.	n.a.	0.90	1.48	0.30	n.a.
	$\langle d \rangle (\text{\AA})$	n.a.	n.a.	4.06	5.20	3.88	n.a.
	$R^2$	n.a.	n.a.	0.9774	0.9967	0.9139	n.a.

# Discussion

Substrate	Parameters	Water	Formamide	Glycerol	Ethylene carbonate	Methylene iodide	Methyl benzoate
Glass	$f$	1.18	1.19	0.53	0.32	1.32	0.56
	$\langle d \rangle (\text{\AA})$	3.56	3.86	5.07	4.80	3.87	4.14
	$R^2$	0.9870	0.9619	0.9683	0.9902	0.8724	0.9863
PTFE	$f$	3.00	0.50	0.84	0.85	0.26	0.71
	$\langle d \rangle (\text{\AA})$	3.60	20.09	9.06	9.73	56.03	9.19
	$R^2$	0.9886	0.9069	0.9695	0.9941	0.7488	0.9375
Stainless steel	$f$	3.25	2.16	1.38	1.83	1.57	0.56
	$\langle d \rangle (\text{\AA})$	3.00	3.67	4.66	4.69	3.70	4.21
	$R^2$	0.9996	0.9716	0.9871	0.9983	0.9880	0.9076
Brass	$f$	2.14	2.16	0.92	2.05	1.36	0.19
	$\langle d \rangle (\text{\AA})$	3.09	3.38	4.96	4.36	3.32	4.33
	$R^2$	0.9898	0.9920	0.9584	0.9841	0.9862	1 (*)
Alumina	$f$	n.a.	1.41	1.20	1.25	1.41	0.09
	$\langle d \rangle (\text{\AA})$	n.a.	4.21	4.99	4.80	3.51	4.96
	$R^2$	n.a.	0.9957	0.9561	0.9998	0.9995	1(*)
Zirconia	$f$	n.a.	n.a.	0.90	1.48	0.30	n.a.
	$\langle d \rangle (\text{\AA})$	n.a.	n.a.	4.06	5.20	3.88	n.a.
	$R^2$	n.a.	n.a.	0.9774	0.9967	0.9139	n.a.

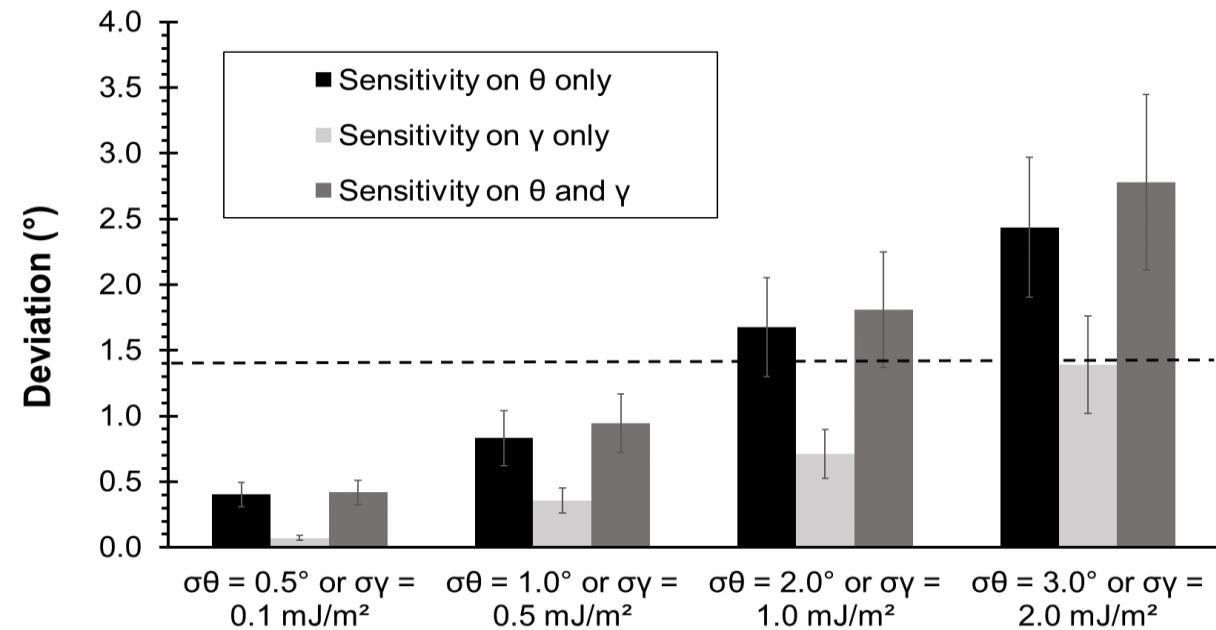
# Discussion

Substrate	Parameters	Water	Formamide	Glycerol	Ethylene carbonate	Methylene iodide	Methyl benzoate
Glass	$f$	1.18	1.19	0.53	0.32	1.32	0.56
	$\langle d \rangle (\text{\AA})$	3.56	3.86	5.07	4.80	3.87	4.14
	$R^2$	0.9870	0.9619	0.9683	0.9902	0.8724	0.9863
PTFE	$f$	3.00	0.50	0.84	0.85	0.26	0.71
	$\langle d \rangle (\text{\AA})$	3.60	20.09	9.06	9.73	56.03	9.19
	$R^2$	0.9886	0.9069	0.9695	0.9941	0.7488	0.9375
Stainless steel	$f$	3.25	2.16	1.38	1.83	1.57	0.56
	$\langle d \rangle (\text{\AA})$	3.00	3.67	4.66	4.69	3.70	4.21
	$R^2$	0.9996	0.9716	0.9871	0.9983	0.9880	0.9076
Brass	$f$	2.14	2.16	0.92	2.05	1.36	0.19
	$\langle d \rangle (\text{\AA})$	3.09	3.38	4.96	4.36	3.32	4.33
	$R^2$	0.9898	0.9920	0.9584	0.9841	0.9862	1 (*)
Alumina	$f$	n.a.	1.41	1.20	1.25	1.41	0.09
	$\langle d \rangle (\text{\AA})$	n.a.	4.21	4.99	4.80	3.51	4.96
	$R^2$	n.a.	0.9957	0.9561	0.9998	0.9995	1(*)
Zirconia	$f$	n.a.	n.a.	0.90	1.48	0.30	n.a.
	$\langle d \rangle (\text{\AA})$	n.a.	n.a.	4.06	5.20	3.88	n.a.
	$R^2$	n.a.	n.a.	0.9774	0.9967	0.9139	n.a.

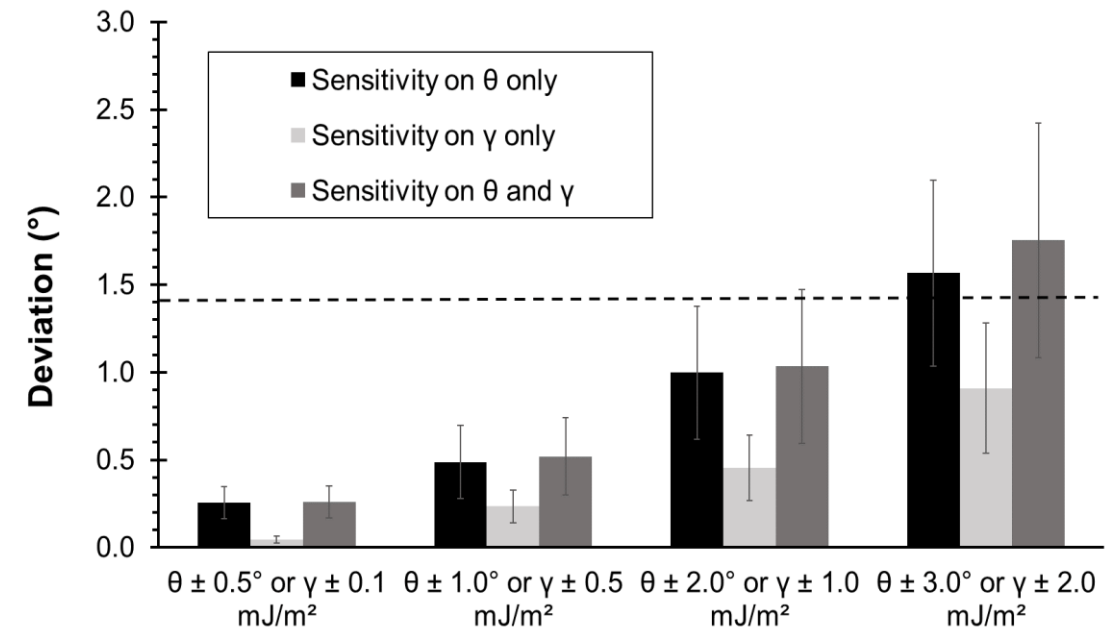
# Discussion

Substrate	Parameters	Water	Formamide	Glycerol	Ethylene carbonate	Methylene iodide	Methyl benzoate
Glass	$f$	1.18	1.19	0.53	0.32	1.32	0.56
	$\langle d \rangle (\text{Å})$	3.56	3.86	5.07	4.80	3.87	4.14
	$R^2$	0.9870	0.9619	0.9683	0.9902	0.8724	0.9863
PTFE	$f$	3.00	0.50	0.84	0.85	0.26	0.71
	$\langle d \rangle (\text{Å})$	3.60	20.09	9.06	9.73	56.03	9.19
	$R^2$	0.9886	0.9069	0.9695	0.9941	0.7488	0.9375
Stainless steel	$f$	3.25	2.16	1.38	1.83	1.57	0.56
	$\langle d \rangle (\text{Å})$	3.00	3.67	4.66	4.69	3.70	4.21
	$R^2$	0.9996	0.9716	0.9871	0.9983	0.9880	0.9076
Brass	$f$	2.14	2.16	0.92	2.05	1.36	0.19
	$\langle d \rangle (\text{Å})$	3.09	3.38	4.96	4.36	3.32	4.33
	$R^2$	0.9898	0.9920	0.9584	0.9841	0.9862	1 (*)
Alumina	$f$	n.a.	1.41	1.20	1.25	1.41	0.09
	$\langle d \rangle (\text{Å})$	n.a.	4.21	4.99	4.80	3.51	4.96
	$R^2$	n.a.	0.9957	0.9561	0.9998	0.9995	1(*)
Zirconia	$f$	n.a.	n.a.	0.90	1.48	0.30	n.a.
	$\langle d \rangle (\text{Å})$	n.a.	n.a.	4.06	5.20	3.88	n.a.
	$R^2$	n.a.	n.a.	0.9774	0.9967	0.9139	n.a.

# Sensitivity analysis: Deviation of the contact angle between simulated values and the “ideal” predicted values



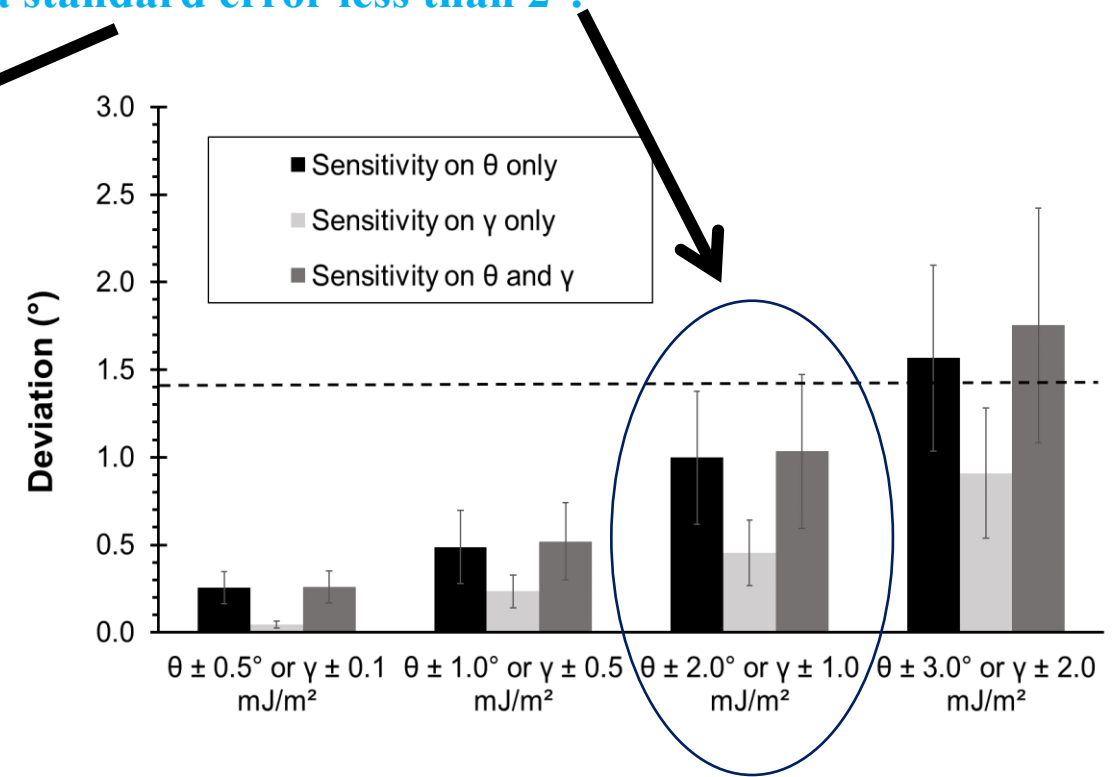
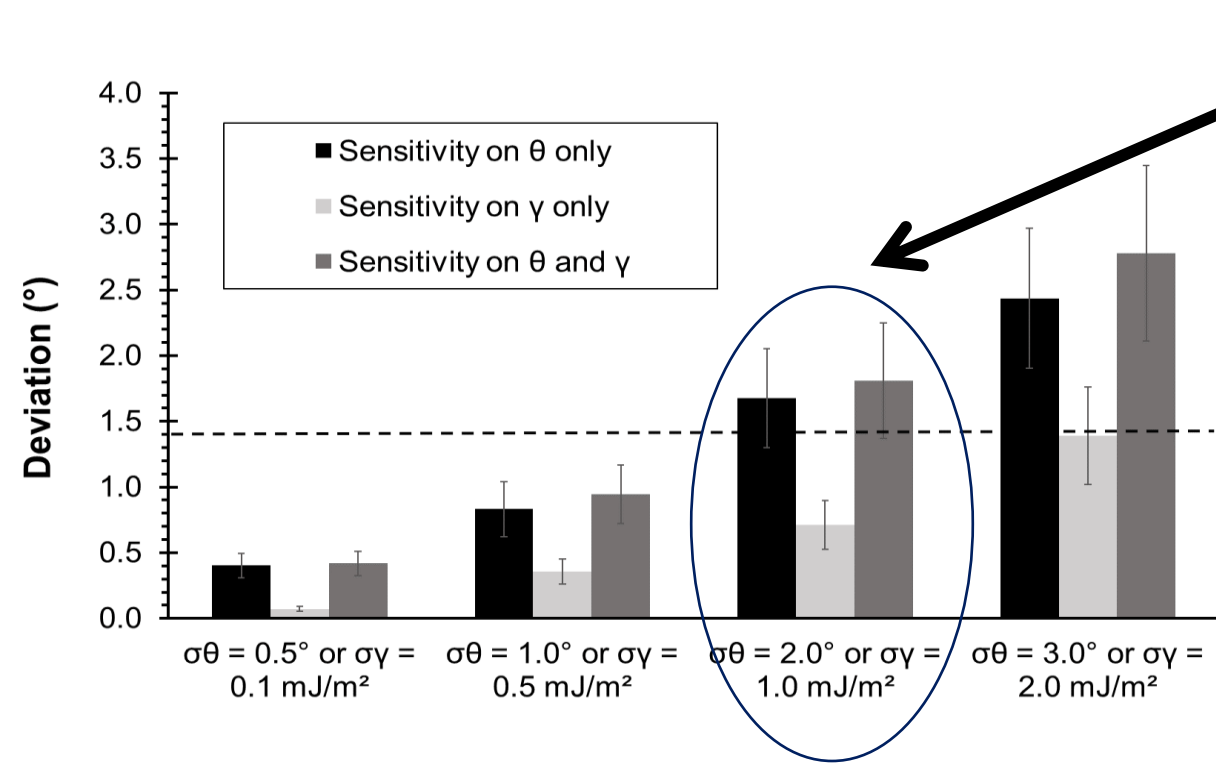
The simulated values were distributed according to a **normal distribution with standard deviations  $\sigma\theta$  and  $\sigma\gamma$** . The simulation was performed in the case of glycerol on steel ( $f = 1.38$  and  $\langle d \rangle = 4.66 \text{ \AA}$ ). The dotted line shows the deviation between our experiment and the ideal case.



Random noise fluctuations around the average values and between lower and upper bounds (“experimental cutoff”).

# Sensitivity analysis: Deviation of the contact angle between simulated values and the “ideal” predicted values

Predictions with a standard error less than 2°.

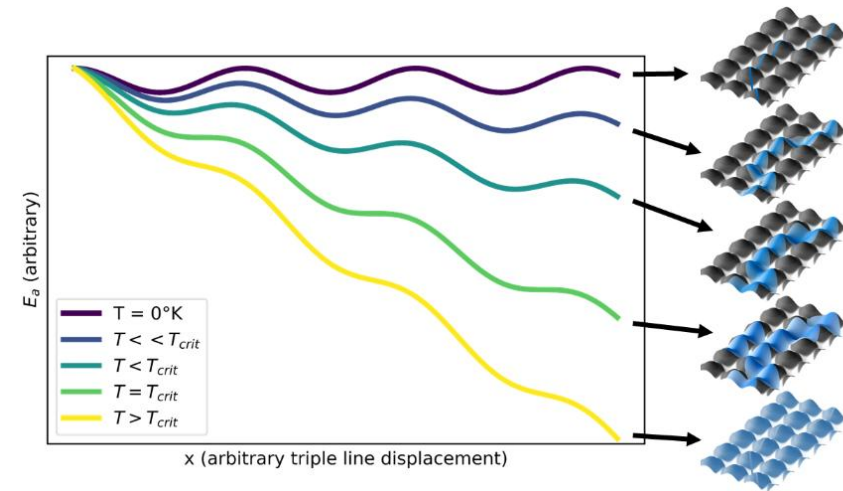


The simulated values were distributed according to a **normal distribution with standard deviations  $\sigma\theta$  and  $\sigma\gamma$** . The simulation was performed in the case of glycerol on steel ( $f = 1.38$  and  $\langle d \rangle = 4.66 \text{ \AA}$ ). The dotted line shows the deviation between our experiment and the ideal case.

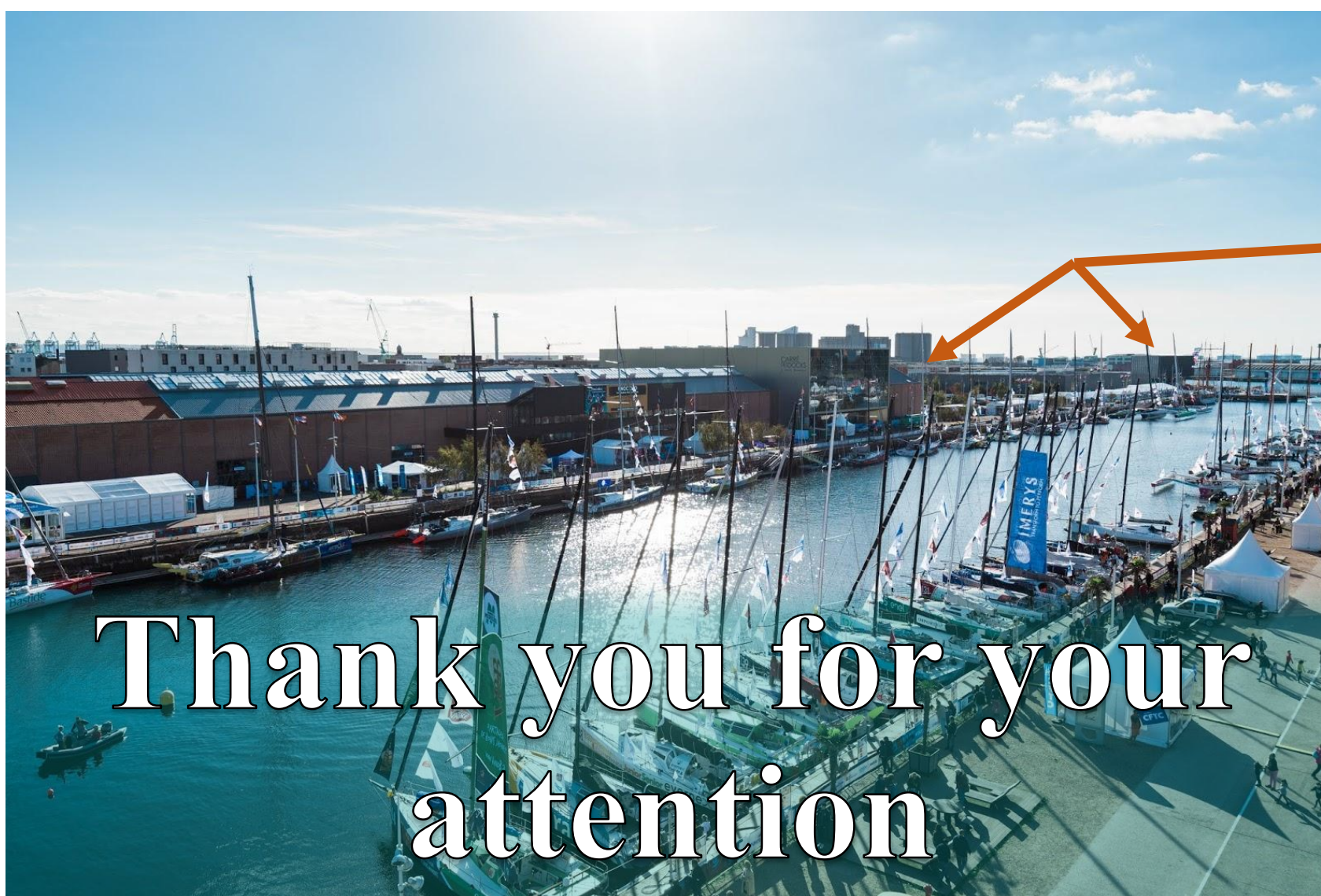
Random noise fluctuations around the average values and between lower and upper bounds (“experimental cutoff”).

# Conclusions

- Predicting contact angle variations with temperature cannot be performed using the partitioning theory.
- A novel physical model is proposed centered around the extension of thermocapillary vibrations near the interface.
- The model is based on scaling arguments.
- The model encompasses normal wetting, Cassie-Baxter and Wenzel states, and the transition to total wetting.
- Temperature variations can be useful to yield two comprehensive parameters:  $f$  and  $\langle d \rangle$
- The novel model appears to predict meaningful contact angles with experimentally realistic noise levels: sensitivity analysis showed that standard deviations  $\sigma_{\theta} = 2^{\circ}$  and  $\sigma_{\gamma} = 1 \text{ mJ/m}^2$  would still produce predicted angles with a standard error less than  $2^{\circ}$ .







LAB

Thank you for your attention

TRANSAT JACQUES VABRE  
([www.scanvoile.com](http://www.scanvoile.com))

THANKS to funding agency: French National Research Agency (grant number ANR-11-RMNP-0020)

Duchemin, B., Cazaux, G., Gomina, M., Bréard, J., 2021. Temperature-dependence of the static contact angle: A transition state theory approach. *Journal of Colloid and Interface Science* 592, 215–226. (Preprint on HAL.)

PAPER ID: 3550191 *The potential of nanocelluloses in microfluidics: Optofluidics, liquid marbles and disposable chips*  
[CELL] SESSION: *Advances in Renewable Materials* ; DATE: April 14, 2021; PRESENTATION TIME: 3:30 PM to 3:55 PM